Proofs and Supplementary Material for paper: Non-Stationary Channel Unified Characterization and Eigenfunction Precoding

Appendix A
Related work

We categorize the related work into three categories:

Characterization of Non-Stationary Channels: Wireless channel characterization in the literature typically require several local and global (in space-time dimensions) higher order statistics to characterize or model non-stationary channels, due to their time-varying statistics. These statistics cannot completely characterize the non-stationary channel, however are useful in reporting certain properties that are required for the application of interest such as channel modeling, assessing the degree of stationarity etc. Contrarily, we leverage the 2-dimensional eigenfunctions that are decomposed from the most generic representation of any wireless channel as a spatio-temporal channel kernel. These spatio-temporal eigenfunctions can be used to extract any higher order statistics of the channel as demonstrated in Section III, and hence serves as a complete characterization of the channel. Furthermore, since this characterization can also generalize to stationary channels, it is a unified characterization for any wireless channel. Beyond characterizing the channel, these eigenfunctions are the core of the precoding algorithm.

Precoding Non-Stationary Channels: Although precoding non-stationary channels is unprecedented in the literature [7], we list the most related literature for completeness. The challenge in precoding non-stationary channels is the lack of accurate models of the channel and the (occasional) CSI feedback does not fully characterize the non-stationarities in its statistics. This leads to suboptimal performance using state-of-the-art precoding techniques like Dirty Paper Coding which assume that complete and accurate knowledge of the channel is available, while the CSI is often outdated in non-stationary channels. While recent literature present attempt to deal with imperfect CSI by modeling the error in the CSI [19], [20], [21], [22], [23], [24], [25], [26], they are limited by the assumption the channel or error statistics are stationary or WSSUS at best. Another class of literature, attempt to deal with the impact of outdated CSI [27], [28] in time-varying channels by quantifying this loss or relying statistical CSI. These methods are not directly suitable for non-stationary channels, as the time dependence of the statistics may render the CSI (or its statistics) stale, consequently resulting in precoding error.

Space-Temporal Precoding: While, precoding has garnered significant research, spatio-temporal interference is typically treated as two separate problems, where spatial precoding at the transmitter aims to cancel inter-user and inter-antenna interference, while equalization at the receiver mitigates inter-carrier and inter-symbol interference. Alternately, [29] proposes to modulate the symbols such that it reduces the cross-symbol interference in the delay-Doppler domain, but requires equalization at the receiver to completely cancel such interference in practical systems. Moreover, this approach cannot completely minimize the joint spatio-temporal interference that occurs in non-stationary channels since their statistics depend on the time-frequency domain in addition to the delay-Dopper domain (explained in Section II). While spatio-temporal block coding techniques are studied in the literature [1] they add redundancy and hence incur a communication overhead to mitigate interference, which we avoid by precoding. These techniques are capable of independently canceling the interference in each domain, however are incapable of mitigating interference that occurs in the joint spatio-temporal domain in non-stationary channels. We design a joint spatio-temporal precoding that leverages the extracted 2-D eigenfunctions from non-stationary channels to mitigate interference that occurs on the joint space-time dimensions, which to the best of our knowledge is unprecedented in the literature.

Appendix B
Results on Interference

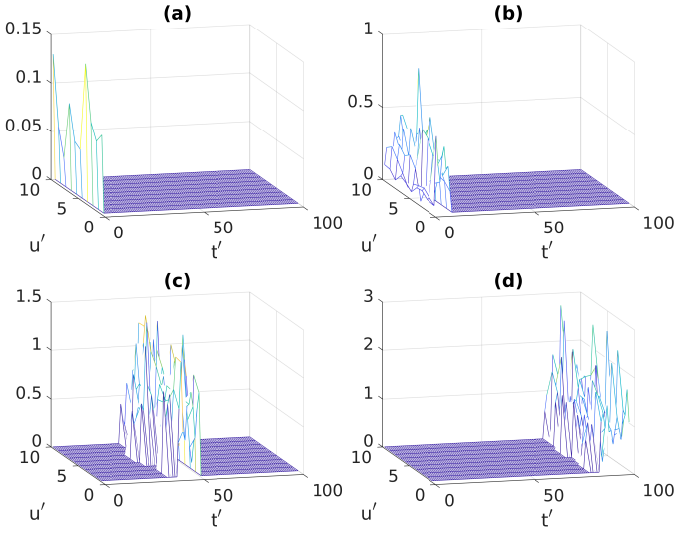

Figure 8: Kernel $k_H(u,t;u',t')$ for u=1 at a) t=1, b) t=10, c) t=50 and d) t=100.

Figure 8 shows the channel response for user u=1 at t=1, t=10, t=50 and t=100, where at each instance, the response for user u=1 is not only affected by its own delay and other users' spatial interference, but also affected by other users' delayed symbols. This is the cause of joint space-time interference which necessitates joint precoding in the 2-dimensional space using eigenfunctions that are jointly orthogonal.

Appendix C
Proofs on Unified Characterization

A. Proof of Lemma 1: Generalized Mercer's theorem

Proof. Consider a 2-dimensional process $K(t,t') \in L^2(Y \times X)$, where $Y(t)$ and $X(t')$are square-integrable zero-mean random processes with covariance function K_Y and K_X, respecly.

Denote the projection of $K(t,t')$ on $X(t')$ as

$$C(t) = \int K(t,t')X(t')\ dt' \tag{30}$$

By *Karhunen–Loève theorem* (KLT), we have

$$X(t') = \sum_{i=1}^{\infty} x_i \phi_i(t') \tag{31}$$

$$C(t) = \sum_{j=1}^{\infty} c_j \psi_j(t) \tag{32}$$

where x_i and z_j are both random variables. $\phi_i(t')$ and $\psi_j(t)$ are eigenfuncions of T_{K_X} and T_{K_C}, respectively.

Notice i and j have the same range, denote $n = i = j$ and $\sigma_n = c_n/x_n$. Let

$$K(t,t') = \sum_{n}^{\infty} \sigma_n \psi_n(t)\phi_n(t') \tag{33}$$

Substituting (31) and (33) at the right side of (30), we have

$$\begin{aligned}
&\int K(t,t')X(t')\ dt' \\
&= \int \sum_{n}^{\infty} \sigma_n \psi_n(t)\phi_n(t') \sum_{n}^{\infty} x_n \phi_n(t')\ dt' \\
&= \int \sum_{n}^{\infty} \sigma_n x_n \psi_n(t) |\phi_n(t')|^2 \\
&+ \sum_{n' \neq n}^{\infty} \sigma_n x_{n'} \psi_n(t)\phi_n(t')\phi^*_{n'}(t')\ dt' \\
&= \sum_{n}^{\infty} c_n \psi_n(t)
\end{aligned} \tag{34}$$

which is equal to the left side of (30). Therefore $K(t,t')$ can be decomposed as (33).

□

B. Proof of Theorem 1: High Order Generalized Mercer's theorem

Proof. Given 2-D process $X(\gamma_1,\gamma_2)$, we have the eigen decomposition by Lemma 1

$$X(\gamma_1,\gamma_2) = \sum_{n}^{\infty} x_n e_n(\gamma_1) s_n(\gamma_2) \tag{35}$$

Let $\psi_n(\gamma_1,\gamma_2) = e_n(\gamma_1)s_n(\gamma_2)$, and substitute in (35), we have

$$X(\gamma_1,\gamma_2) = \sum_{n}^{\infty} x_n \phi_n(\gamma_1,\gamma_2) \tag{36}$$

where $\phi_n(\gamma_1,\gamma_2)$ is 2-D eigenfunctions with

$$\iint \phi_n(\gamma_1,\gamma_2)\phi_{n'}(\gamma_1,\gamma_2)\ d\gamma_1\ d\gamma_2 = \delta_{nn'} \tag{37}$$

Notice (36) is 2-D KLT. With iterations of above steps, we get *High Order KLT* for $X(\gamma_1,\cdots,\gamma_Q)$ and $C(\zeta_1,\cdots,\zeta_P)$

$$X(\gamma_1,\cdots,\gamma_Q) = \sum_{n}^{\infty} x_n \phi_n(\gamma_1,\cdots,\gamma_Q) \tag{38}$$

$$C(\zeta_1,\cdots,\zeta_P) = \sum_{n}^{\infty} c_n \psi_n(\zeta_1,\cdots,\zeta_P) \tag{39}$$

where $C(\zeta_1,\cdots,\zeta_P)$ is the projection of $X(\gamma_1,\cdots,\gamma_Q)$ on $K(\zeta_1,\cdots,\zeta_P;\gamma_1,\cdots,\gamma_Q)$.

Then follows the similar steps in Appendix C-A, we can get

$$\begin{aligned}
&K(\zeta_1,\cdots,\zeta_P;\gamma_1,\cdots,\gamma_Q) \\
&= \sum_{n}^{\infty} \sigma_n \psi_n(\zeta_1,\cdots,\zeta_P)\phi_n(\gamma_1,\cdots,\gamma_Q)
\end{aligned} \tag{40}$$

□

APPENDIX D
PROOFS ON EIGENFUNCTION BASED PRECODING

A. Proof of Lemma 2

Proof. By KLT, $x(u,t)$ can be expressed as

$$x(u,t) = \sum_{n}^{\infty} x_n \phi_n(u,t) \tag{41}$$

where x_n is random variable with $E\{x_n x_{n'}\} = \lambda_n \sigma_{nn'}$ and $\phi_n(u,t)$ is 2-D eigenfunction.

Denote $c_n(u,t)$ as the projection of $k_H(u,t;u',t')$ on $\phi_n(u',t')$

$$c_n(u,t) = \iint k_H(u,t;u',t')\phi_n(u',t')\ du'\ dt' \tag{42}$$

Then (25) can be expressed as

$$\begin{aligned}
&||s(u,t) - Hx(u,t)||^2 \\
&= ||s(u,t) - \sum_{n}^{\infty} x_n c_n(u,t)||^2
\end{aligned} \tag{43}$$

Let $\epsilon(x) = ||s(u,t) - \sum_n^{\infty} x_n \phi_n(u,t)||^2$, the expansion is

$$\begin{aligned}
\epsilon(x) &= \langle s,s\rangle - 2\sum_{n}^{\infty} x_n \langle c_n, s\rangle + \sum_{n}^{\infty} x_n^2 \langle c_n, c_n\rangle \\
&+ \sum_{n}^{\infty}\sum_{n'\neq n}^{\infty} x_n x_{n'} \langle c_n, c'_n\rangle
\end{aligned} \tag{44}$$

Solve $\frac{\partial \epsilon(x)}{\partial x_n} = 0$, we get the solution

$$x_n^{opt} = \frac{\langle s, c_n\rangle + \sum_{n'\neq n}^{\infty} x_{n'}\langle c_{n'}, c_n\rangle}{\langle c_n, c_n\rangle} \tag{45}$$

where $\langle a,b\rangle = \int a(u,t)b^*(u,t)\ du\ dt$ is the inner product.

Let $\langle c_{n'}, c_n\rangle = 0$, i.e., the projections $\{c_n(u,t)\}_n$ are orthogonal basis, we have closed form x^{opt}

$$x_n^{opt} = \frac{\langle s, c_n\rangle}{\langle c_n, c_n\rangle} \tag{46}$$

Substitute (46) in (44), easily get $\epsilon(x) = 0$. □

B. Proof of Theorem 2: Eigenfunction Precoding

Proof. From *Theorem 1*, the kernel $k_H(u,t;u',t')$ can be decomposed to two separate eigenfunction sets. Propagate eigenfunction trough channel H, we have

$$H\phi_n^*(u,t) = \iint k_H(u,t;u',t')\phi_n^*(u',t')\ du'\ dt'$$

$$
\begin{aligned}
&= \iint \sum_{n}^{\infty} \{\sigma_n \psi_n(u,t)\phi_n(u',t')\} \phi_n^*(u',t') \; dt' \; df' \\
&= \iint \sigma_n \psi_n(u,t) |\phi_n(u',t')|^2 \\
&+ \sum_{n' \neq n}^{\infty} \sigma_{n'} \psi_{n'}(u,t) \phi_{n'}(u',t') \; \phi_n^*(u',t') \; du' \; dt' \\
&= \sigma_n \psi_n(u,t) \qquad (47)
\end{aligned}
$$

where $\psi_n(u,t)$ is eigenfunction and has orthogonal property.

From *lemma 2*, the eigenfunction projection would give us optimal solution. Let $x(u,t)$ be the linear combination of $\{\phi_n^*(u,t)\}$ with coefficients $\{x_n\}$.

$$
x(u,t) = \sum_{n}^{\infty} x_n \phi_n^*(u,t) \qquad (48)
$$

Then we have

$$
\begin{aligned}
&\arg\min_{x(u,t)} ||s(u,t) - Hx(u,t)||^2 \\
&= \arg\min_{\{x_n\}} ||s(u,t) - \sum_{n}^{\infty} x_n \sigma_n \psi_n(u,t)||^2 \qquad (49)
\end{aligned}
$$

Optimal x_n can be obtained by

$$
x_n^{opt} = \frac{\langle s(u,t), \psi_n(u,t) \rangle}{\sigma_n} \qquad (50)
$$

Substitute (50) in (48), the transmit signal is designed as

$$
x(u,t) = \sum_{n}^{\infty} \frac{\langle s(u,t), \psi_n(u,t) \rangle}{\sigma_n} \phi_n^*(u,t) \qquad (51)
$$

□

C. Proof of Corollary 1

Proof. The kernel $K_H(u,u')$ is 2-D case of Theorem 2, and proof steps are the same with Appendix D-B. □

APPENDIX E
IMPLEMENTATION SUPPLEMENT

For 4-D kernel tensor $\mathbf{K} \in \mathrm{C}^{N_u \times T \times N_u \times T}$ and 2-D symbol vectors $\mathbf{r}, \mathbf{x} \in \mathrm{C}^{N_u \times T}$, we have the I/O relation (noise-free)

$$
\mathbf{r}[u,t] = \sum_{u'=1}^{N_u} \sum_{t'=1}^{T} \mathbf{K}[u,t;u',t'] \mathbf{x}[u',t'] \qquad (52)
$$

where $[\cdot]$ denote the entry. N_u and T is the number of users and time instances, respectively. Through invertible mapping $f{:}u \times t \to m$, we have $\mathbf{K} \in \mathrm{C}^{N_u T \times N_u T}$ and $\mathbf{r}, \mathbf{x} \in \mathrm{C}^{N_u T \times 1}$. The I/O relation becomes

$$
\mathbf{r}[m] = \sum_{m'=1}^{N_u T} \mathbf{K}[m;m'] \mathbf{x}[m'] \qquad (53)
$$

which is matrix multiplication $\mathbf{r}{=}\mathbf{K}\mathbf{x}$. Split $\mathbf{r}$, $\mathbf{K}$ and $\mathbf{x}$ to real parts $\mathbf{R}$ and imaginary parts $\mathbf{I}$, respectively. We can construct new kernel matrix and symbols vectors $\mathbf{r}' = \begin{bmatrix} \mathbf{R_r} \\ \mathbf{I_r} \end{bmatrix}$, $\mathbf{K}' = \begin{bmatrix} \mathbf{R_K} & -\mathbf{I_K} \\ \mathbf{I_K} & \mathbf{R_K} \end{bmatrix}$ and $\mathbf{x}' = \begin{bmatrix} \mathbf{R_x} \\ \mathbf{I_x} \end{bmatrix}$ with same I/O relation $\mathbf{r}' = \mathbf{K}'\mathbf{x}'$ due to linear relation

$$
\begin{bmatrix} \mathbf{R_r} \\ \mathbf{I_r} \end{bmatrix} = \begin{bmatrix} \mathbf{R_K} & -\mathbf{I_K} \\ \mathbf{I_K} & \mathbf{R_K} \end{bmatrix} \times \begin{bmatrix} \mathbf{R_x} \\ \mathbf{I_x} \end{bmatrix} \qquad (54)
$$

Thus the complex space converts to real space, with the size of kernel matrix and symbol vectors increases as $\mathbf{K}' \in \mathrm{C}^{2N_u T \times 2N_u T}$ and $\mathbf{r}', \mathbf{x}' \in \mathrm{C}^{2N_u T \times 1}$, which means number of basis increased. For the real space I/O relation, $\mathbf{x}'$ can be obtained by HOGMT-precoding with $\mathbf{K}'$ and $\mathbf{s}'$ ($\mathbf{s}'$ can also be obtained by the same mapping, split and construction).

Then combine real and imaginary parts $\mathbf{x} = \mathbf{R_x} + i\mathbf{I_x}$, and do inverse mapping $g{:}m \to u \times t$, we get the final precoded signal vector $\mathbf{x}[u,t]$. The implementation data flow is shown as Figure 9.

Figure 10a and Figure 10b show the BER performance of HOGMT based spatial precoding and space-time precoding with $\epsilon{=}10^{-3}$ for BPSK, QPSK, 16QAM and 64QAM modulation, respectively.

REFERENCES

[1] Y. S. Cho, J. Kim, W. Y. Yang, and C. G. Kang, *MIMO-OFDM Wireless Communications with MATLAB*. Wiley Publishing, 2010.

[2] N. Fatema, G. Hua, Y. Xiang, D. Peng, and I. Natgunanathan, "Massive mimo linear precoding: A survey," *IEEE systems journal*, vol. 12, no. 4, pp. 3920–3931, 2017.

[3] M. Costa, "Writing on dirty paper (corresp.)," *IEEE Transactions on Information Theory*, vol. 29, no. 3, pp. 439–441, 1983.

[4] C.-X. Wang, J. Bian, J. Sun, W. Zhang, and M. Zhang, "A survey of 5g channel measurements and models," *IEEE Communications Surveys & Tutorials*, vol. 20, no. 4, pp. 3142–3168, 2018.

[5] Z. Huang and X. Cheng, "A general 3d space-time-frequency non-stationary model for 6g channels," *IEEE Transactions on Wireless Communications*, vol. 20, no. 1, pp. 535–548, 2020.

[6] C. F. Mecklenbrauker, A. F. Molisch, J. Karedal, F. Tufvesson, A. Paier, L. Bernadó, T. Zemen, O. Klemp, and N. Czink, "Vehicular channel characterization and its implications for wireless system design and performance," *Proceedings of the IEEE*, vol. 99, no. 7, pp. 1189–1212, 2011.

[7] A. Ali, E. D. Carvalho, and R. W. Heath, "Linear receivers in non-stationary massive mimo channels with visibility regions," *IEEE Wireless Communications Letters*, vol. 8, no. 3, pp. 885–888, 2019.

[8] R. Hadani, S. Rakib, S. Kons, M. Tsatsanis, A. Monk, C. Ibars, J. Delfeld, Y. Hebron, A. J. Goldsmith, A. F. Molisch, and A. R. Calderbank, "Orthogonal time frequency space modulation," *CoRR*, vol. abs/1808.00519, 2018. [Online]. Available: http://arxiv.org/abs/1808.00519

[9] G. Matz and F. Hlawatsch, "Time-varying communication channels: Fundamentals, recent developments, and open problems," in *2006 14th European Signal Processing Conference*, 2006, pp. 1–5.

[10] F. Hlawatsch and G. Matz, *Wireless Communications Over Rapidly Time-Varying Channels*, 1st ed. USA: Academic Press, Inc., 2011.

[11] M. Pätzold and C. A. Gutierrez, "Modelling of non-wssus channels with time-variant doppler and delay characteristics," in *2018 IEEE Seventh International Conference on Communications and Electronics (ICCE)*, 2018, pp. 1–6.

[12] J. Bian, C.-X. Wang, X. Gao, X. You, and M. Zhang, "A general 3d non-stationary wireless channel model for 5g and beyond," 2021.

[13] A. D. Zhibin Zou, Maqsood Careem and N. Thawdar, "Appendix for unified characterization and precoding fornon-stationary channels." [Online]. Available: https://www.dropbox.com/s/iu6e9hh3h2xsc8m/ICC22_NS_Precoding_Proof.pdf?dl=0

[14] G. Matz, "On non-wssus wireless fading channels," *IEEE Transactions on Wireless Communications*, vol. 4, no. 5, pp. 2465–2478, 2005.

[15] J. Mercer, "Functions of positive and negative type, and their connection with the theory of integral equations," *Philosophical Transactions of the Royal Society of London. Series A, Containing Papers of a Mathematical or Physical Character*, vol. 209, pp. 415–446, 1909. [Online]. Available: http://www.jstor.org/stable/91043

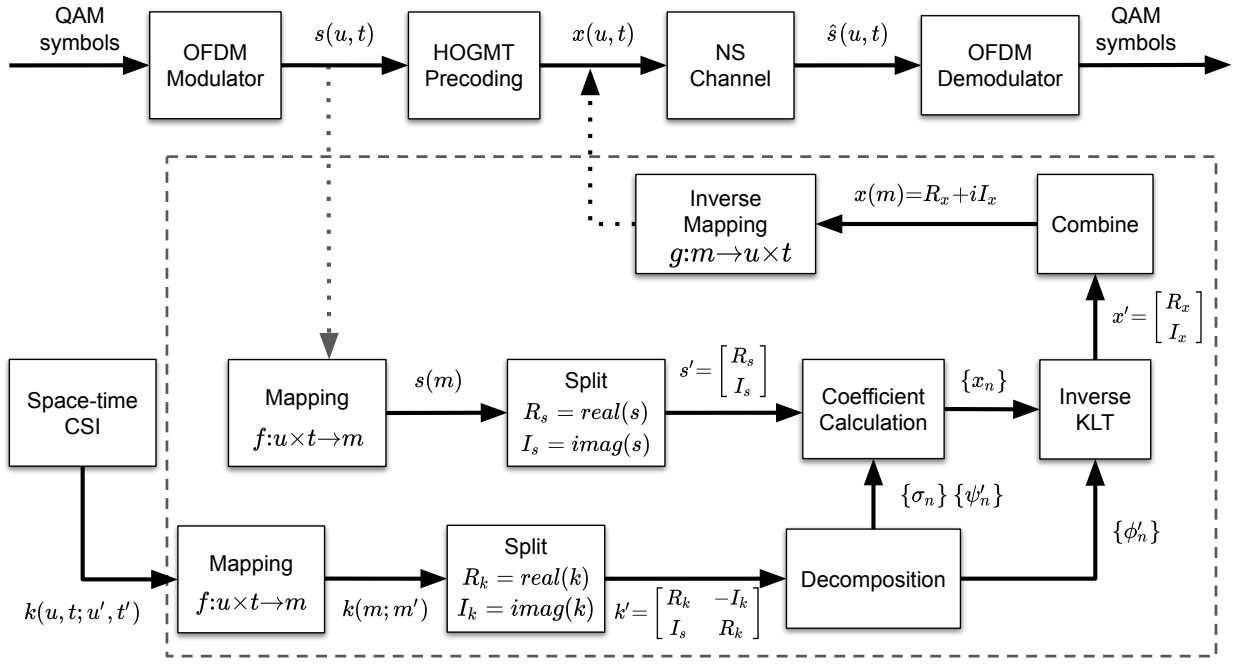

Figure 9: Data flow

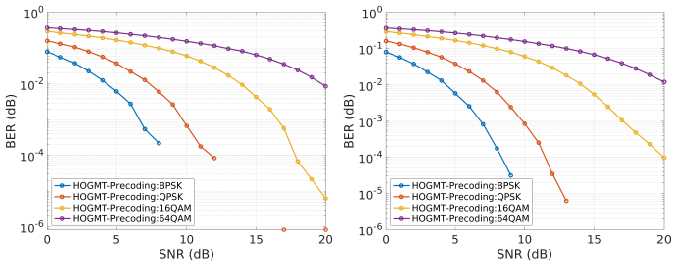

(a) BER of HOGMT based spatial precoding (b) BER of HOGMT based spatio-temporal precoding

Figure 10: BER of HOGMT based precoding with $\epsilon{=}10^{-3}$ for BPSK, QPSK, 16QAM and 64QAM

[16] L. Wang, *Karhunen-Loeve expansions and their applications*. London School of Economics and Political Science (United Kingdom), 2008.

[17] G. Matz, "Doubly underspread non-wssus channels: analysis and estimation of channel statistics," in *2003 4th IEEE Workshop on Signal Processing Advances in Wireless Communications - SPAWC 2003 (IEEE Cat. No.03EX689)*, 2003, pp. 190–194.

[18] M. H. Vu, "Exploiting transmit channel side information in mimo wireless systems," Ph.D. dissertation, Stanford University, 2006.

[19] Y. Hatakawa, T. Matsumoto, and S. Konishi, "Development and experiment of linear and non-linear precoding on a real-time multiuser-mimo testbed with limited csi feedback," in *2012 IEEE 23rd International Symposium on Personal, Indoor and Mobile Radio Communications - (PIMRC)*, 2012, pp. 1606–1611.

[20] F. Hasegawa, H. Nishimoto, N. Song, M. Enescu, A. Taira, A. Okazaki, and A. Okamura, "Non-linear precoding for 5g nr," in *2018 IEEE Conference on Standards for Communications and Networking (CSCN)*, 2018, pp. 1–7.

[21] X. Guo, D. Yang, Z. Luo, H. Wang, and J. Kuang, "Robust thp design for energy efficiency of multibeam satellite systems with imperfect csi," *IEEE Communications Letters*, vol. 24, no. 2, pp. 428–432, 2020.

[22] F. A. Dietrich, P. Breun, and W. Utschick, "Robust tomlinson–harashima precoding for the wireless broadcast channel," *IEEE Transactions on Signal Processing*, vol. 55, no. 2, pp. 631–644, 2007.

[23] D. Castanheira, A. a. Silva, and A. Gameiro, "Linear and nonlinear precoding schemes for centralized multicell mimo-ofdm systems," *Wirel. Pers. Commun.*, vol. 72, no. 1, p. 759–777, Sep. 2013. [Online]. Available: https://doi.org/10.1007/s11277-013-1041-z

[24] R. Wang, M. Tao, and Z. Xiang, "Nonlinear precoding design for mimo amplify-and-forward two-way relay systems," *IEEE Transactions on Vehicular Technology*, vol. 61, no. 9, pp. 3984–3995, 2012.

[25] M. Mazrouei-Sebdani, W. A. Krzymień, and J. Melzer, "Massive mimo with nonlinear precoding: Large-system analysis," *IEEE Transactions on Vehicular Technology*, vol. 65, no. 4, pp. 2815–2820, 2016.

[26] S. Jacobsson, G. Durisi, M. Coldrey, T. Goldstein, and C. Studer, "Quantized precoding for massive mu-mimo," *IEEE Transactions on Communications*, vol. 65, no. 11, pp. 4670–4684, 2017.

[27] A. L. Anderson, J. R. Zeidler, and M. A. Jensen, "Reduced-feedback linear precoding with stable performance for the time-varying mimo broadcast channel," *IEEE Journal on Selected Areas in Communications*, vol. 26, no. 8, pp. 1483–1493, 2008.

[28] W. Zeng, C. Xiao, M. Wang, and J. Lu, "Linear precoding for finite-alphabet inputs over mimo fading channels with statistical csi," *IEEE Transactions on Signal Processing*, vol. 60, no. 6, pp. 3134–3148, 2012.

[29] R. Hadani, S. Rakib, S. Kons, M. Tsatsanis, A. Monk, C. Ibars, J. Delfeld, Y. Hebron, A. J. Goldsmith, A. F. Molisch, and R. Calderbank, "Orthogonal time frequency space modulation," 2018.